

# DEVELOPMENT OF A FINITE ELEMENT MODEL OF THE HUMAN NECK FOR WHIPLASH SIMULATION

**Seiichi Kobayashi**

**Yuichi Kitagawa**

NISSAN MOTOR CO., LTD.

Japan

Paper Number: 208

## ABSTRACT

A finite element model of the human neck that consists of the vertebral bodies, internal discs, ligaments and muscles has been developed in this study. Not only representing the precise geometry of the human body parts, this study also focused on the muscular response during impacts. A spring-dashpot model has been introduced to activate muscle elements in the head-neck-thorax complex. The evaluation process of the model was divided into two steps. In the first step, the head responses of the neck model were examined while the input was given to the T1 motion and some other connecting points. The complete upper body motion was simulated in the second step by modeling a seat system mounted on a sled. The simulation results showed good agreement with the experimental data and suggested that the model well simulates the head and neck kinematics and responses.

## INTRODUCTION

Many efforts have been made to reduce the cost and period of car design by adopting virtual tests before making prototypes and by using design optimization. Owing to such demands, development of computational technology has been accelerated during the last couple of decades. Numerical simulations are now widely used in automobile industries. Among various methods of numerical simulations, finite element method (FEM) has been widely used with its

advantage in visualization and accuracy. Now finite element simulations are adopted in most design sections despite the fact they require heavy computational resources such as CPU power, memory size and disk space. There is a great benefit in using them especially for an area of car crash safety in terms of reducing the number of expensive crash tests.

A new challenge in finite element simulations in an area of crash safety is real human modeling. The model must be carefully validated against human body kinematics and responses under various impact conditions, in order to simulate injury. Whiplash injuries, which are mostly observed in low-speed rear-end collisions, are becoming an important issue in crash safety area. According to recent insurance statistical data on automobile accidents in Japan, approximately 50% of car-to-car crashes have resulted in neck injuries, particularly at low impact speeds. Despite its frequency, the mechanism of whiplash injuries is not completely understood. A possible mechanism hypothesized by some researchers was that whiplash injuries could occur within the physiological range of neck motion<sup>[1], [2], [3]</sup>.

Human neck models have been developed to examine the validity of hypothesis and to better understand injury mechanisms<sup>[4], [5], [6]</sup>. The most difficult point in neck modeling is to reproduce muscular activities during impacts. Because there are numerous muscles involved in neck motion and rear-end collisions sometimes last long enough to generate muscular reactions, kinematics and responses of the occupant's neck is greatly affected by physiological factors. Among several approaches in muscle modeling, Wittek et al. has successfully simulated the neck motion by introducing a Hill-type model<sup>[7]</sup>. They also obtained different responses with and without muscular tension that could suggest a

possible difference in injury level between occupants who is aware of a collision and who is not. Timing of muscle activation should be carefully controlled with respect to the impact conditions. In this study, a simplified method was adopted for muscle modeling. In order to reproduce muscle responses during impacts, force-elongation curves were directly applied to spring-dashpot elements. By controlling the magnitude and profile of function curves, it became possible to study contribution of the neck muscles as well as to simulate the neck motion in rear impacts.

## MODEL DESCRIPTION

### Overview

The structure of the entire model is shown in Figure 1, which is LABMAN model and used as the base in the first step of validation. Hereafter, we call it base model. Its geometry is based on an average adult male, and its physical properties were defined by being referred to literature data of LAB (Laboratoire d'Accidentologie et de Biomecanique). In the simplified model for the first validation study, soft tissue parts were removed because the load was directly applied to the torso instead of considering a contact with the seat back, as many researchers did. The other features including the geometries and physical

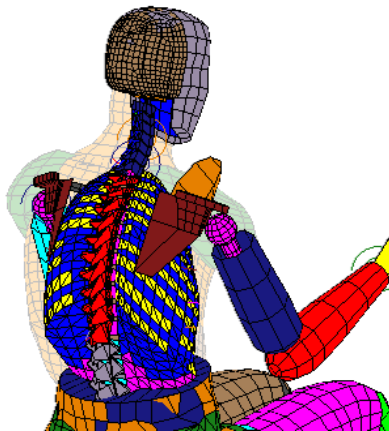
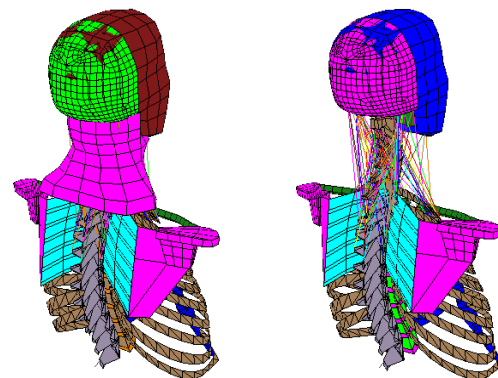


**Figure 1. Base entire human model.**

properties were defined so as to be duplicated the base model. Figure 2 compares the simplified human model just taken out of the base model and the revised one with newly introduced muscle elements. In the base model, the possibility of passive muscular responses not to represent each neck muscular function has been evaluated. On the other hand, one hundred and sixty one spring-dashpot elements were used to represent the neck muscles in the revised model. Their constitution and mechanical properties were carefully defined by making reference to anatomy textbooks.



(a) Base(solid, shell) (b) Revised(spring-dashpot)

**Figure 2. Comparison between base and revised muscle model in the simplified human model.**

### Modeling of Neck Muscles

In the revised human neck model, responses and restrictions in head-neck kinematics are controlled by a total amount of 161 spring-dashpot elements

**Table 1.  
Classified muscle element groups**

Levator Scapulae	Rectus Capitis Anterior
Trapezius Descendens	Lumped Hyoid
Trapezius transversa	Multifidus Cervicis
Sternocleidomastoid	Splenius Capitis
Scalenus Anterior	Splenius Cervicis
Scalenus Midius	Semispinaills Capitis
Scalenus Posterior	Semispinaills Cervicis
Longus Capitis	Longissimus Capitis
Longus Colli Vertical	Longissimus Cervicis
Longus Colli Oblique Inferior	

representing the neck muscles with finite section area as illustrated in Figure 2-(b). The elements can be classified into 19 groups, as shown in Table 1, which are corresponding to anatomical classification. For each muscle group, mechanical properties were characterized based on a Hill-type algorithm as described by<sup>[8]</sup>

$$\mathbf{F} = \underbrace{\mathbf{F}_{CE}}_{\text{Active}} + \underbrace{\mathbf{F}_{PE} + \mathbf{F}_{DE}}_{\text{Passive}} \quad (1),$$

where  $\mathbf{F}$  is the total amount of muscular force working at two ends of a spring-dashpot element and  $\mathbf{F}_{CE}$  is a component representing an active muscular force such as conscious bracing, while the later two components  $\mathbf{F}_{PE}$  and  $\mathbf{F}_{DE}$  represent passive muscular forces. These components can be characterized with respect to living human responses as follows.

$$\mathbf{F}_{CE}(t, \delta, v_n) = N_a(t) \cdot \mathbf{F}_l(\delta) \cdot \mathbf{F}_v(v_n) \quad (2).$$

$$\mathbf{F}_{PE}(\delta) = F_{\max} \cdot \mathbf{F}_p(\delta) \quad (3).$$

$$\mathbf{F}_{DE}(\dot{\delta}) = C_{\text{damp}} \cdot \dot{\delta} \quad (\text{Linear Damper}) \quad (4).$$

In above equations,  $t$ ,  $\delta$  and  $\dot{\delta} \Rightarrow v$  are time, elongation of a muscular and elongation rate respectively.  $F_{\max}$  in Equation (3) indicates the maximum contraction force which the muscle can generate. The function  $\mathbf{F}_p(\delta)$ , which represents a relationship between muscular elongation  $\delta$  and normalized muscular force  $\mathbf{F}_p$ , can be given as an exponential function with respect to a non-dimensional value  $\delta/L_{\text{ofib}}$ , where  $L_{\text{ofib}}$  is the initial muscular length. The viscoelastic effects of muscles are taken into account by a linear dashpot, having a constant coefficient  $C_{\text{damp}}$ , with respect to elongation rate  $\dot{\delta}$ .

Active responses of muscles are characterized by three factors as shown in Equation (2). The first factor  $N_a(t)$  determines the state of muscle activity, which is given as a value between 0.0 and 1.0. The second factor  $\mathbf{F}_l(\delta)$  is a function showing a relationship between muscular elongation and

normalized muscular force. The last one  $\mathbf{F}_v(v_n)$  gives a magnitude of muscular force with respect to elongation rate  $v = \dot{\delta}$ . Namely, these factors can be described by the following equations:

$$N_a = \begin{cases} A_{\text{init}} & , t \leq T_{\text{ref}} \\ A_{\text{init}} + (1 - A_{\text{init}}) \left( 1 + \frac{E_{\text{init}} \cdot T_{\text{nc}} - T_a}{(T_a - T_{\text{nc}}) \exp\left(\frac{t - T_{\text{ref}}}{T_a}\right)} + \frac{T_{\text{nc}}(1 - E_{\text{init}})}{(T_a - T_{\text{nc}}) \exp\left(\frac{t - T_{\text{ref}}}{T_{\text{nc}}}\right)} \right) & \text{in } t > T_{\text{ref}} \end{cases} \quad (5),$$

$$\mathbf{F}_l(\delta) = F_{\max} \cdot \mathbf{F}_l(\delta), \quad \text{where}$$

$$\mathbf{F}_l(\delta) = \exp \left\{ - \left( \frac{\delta + L_{\text{ofib}}(1 - aL_{\text{opt}})}{C_{\text{sh}} \cdot aL_{\text{opt}} \cdot L_{\text{ofib}}} \right)^2 \right\} \quad (6),$$

$$\mathbf{F}_v(v_n) = \begin{cases} 0, & v_n \leq -1 \\ \frac{C_{\text{short}}(1 + v_n)}{C_{\text{short}} - v_n}, & v_n \leq 0 \\ \frac{C_{\text{leng}} + C_{\text{mvl}} \cdot v_n}{C_{\text{leng}} + v_n}, & v_n > 0 \end{cases} \quad (7),$$

where  $t$  means real time,  $T_{\text{ref}}$  is a reflex time,  $A_{\text{init}}$  means the initial active state and  $E_{\text{init}}$  is the initial excitation level. At a reference state,  $E_{\text{init}}$  is equal to  $A_{\text{init}} \cdot T_{\text{nc}}$  and  $T_a$  are time coefficients related to excitation and activation respectively. Figure 3-(a) shows variation of  $N_a(t)$  given by Equation (6) with respect to a response time  $t$ .  $aL_{\text{opt}}$  is a parameter representing the ratio when the muscle generates its maximum contraction force.  $C_{\text{sh}}$  is a shape function describing a relationship between elongation  $\delta$  and muscular force  $\mathbf{F}_l$  as shown in Figure 3-(b).  $v_n$  is a non-dimensional value, which is derived from dividing a real elongation rate  $v$  by a maximum shortening velocity  $v_{\max}$ .  $C_{\text{short}}$ ,  $C_{\text{leng}}$  and  $C_{\text{mvl}}$  are the

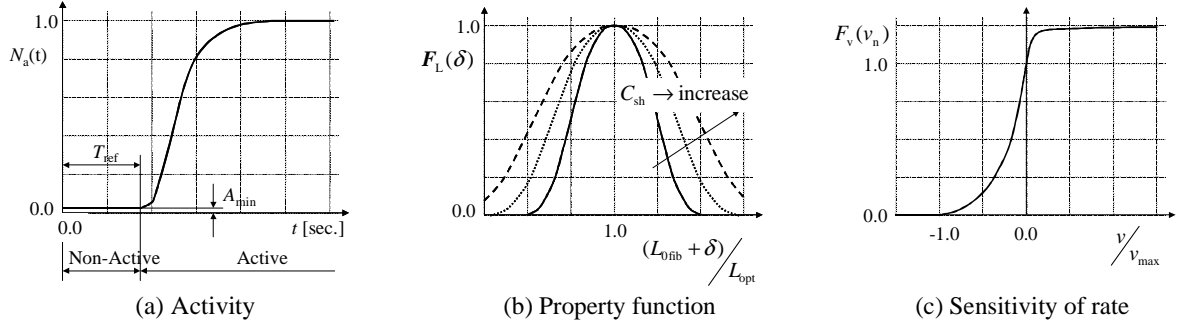


**Figure 3. Muscle property function at active response.**

parameters related to muscular contraction, elongation and maximum force limit respectively. Figure 3-(c) shows the relationship between  $v_n$  and  $F_v(v_n)$ .

As mentioned above, mechanical properties of muscular elements are described by Equation (1) while typical features in active response are known by function curves in Figure 3. Assuming that viscoelastic effects can be neglected by  $F_v(v_n) = 1$  and  $F_{DE} = \mathbf{O}$ , force-elongation characteristics in muscular elements are drawn as function curves in Figure 4.

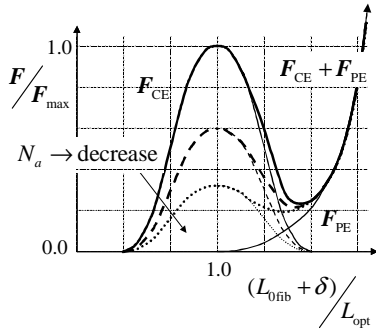


**Figure 4. Response of muscles model.**

In this study, non-linear viscoelastic characteristics were given to spring-dashpot elements so that they could clearly represent mechanical responses of the neck muscles. The following three situations were considered to simplify the functions for muscle elements especially in active responses as shown in Figure 3-(a).

1. Cadaver ( $N_a(t) = 0$ )
2. Human without Notice ( $N_a(t) = 0.05 \square 0.1$ )

### 3. Human with Notice ( $0.1 < N_a(t) \leq 1.0$ )

Among above situations,  $F_{CE}$  in Equation (1) becomes zero in the first case, where all the effects related to this component described in Equation (5) to (7) are neglected. In the later two situations, the living human effects, which are described in Equation (6) and (7), should be introduced. In this study,  $F_v(v_n)$  was assumed to be 1.0 for simplicity, which eliminates effects of  $F_{CE}$  at negative and high rate of  $v_n$ . One reason for this assumption is that it is convenient to separate the responses related to  $F_{CE}$  with respect to different situations as listed above. The other reason comes from difficulties in handling spring-dashpot elements in each numerical analysis code. A general form of nonlinear characteristics for spring-dashpot elements are expressed by

$$F(\delta, \dot{\delta}) = f(\delta) \times \left\{ A + B \ln \left( \frac{\dot{\delta}}{D} \right) + g(\dot{\delta}) \right\} + C \dot{\delta} \quad (8),$$

where elastic component  $\delta$ , viscous component  $\dot{\delta} \Rightarrow v$  and linear viscous component  $C \dot{\delta}$  are included. On the other hand, the form of spring-dashpot element described in Equation (1) can be summarized as follows.

$$F = \underbrace{N_a(t) \cdot F_l(\delta) \cdot F_v(\dot{\delta})}_{\text{Active Property Spring}} + \underbrace{F_{\max} \cdot F_p(\delta) + C_{\text{damp}} \cdot \dot{\delta}}_{\text{Passive Property Spring}} \quad (9).$$

Considering the general form of spring-dashpot element,

it is reasonable to divide the component  $F_{CE}$  into two parts, active and passive components, so as to be described using the linear formation in Equation (9). In addition, it is assumed that  $F_v(v_n) = 0$  and  $C_{damp} \cdot \dot{\delta} = 0$  for simplicity in the following simulation.

## MODEL VALIDATION

### Rear Impact Test

A dataset was taken from a series of rear impact tests conducted at JARI (Japan Automobile Research Institute) in the NISSAN-JARI whiplash project (1998). The subject, a human volunteer, was asked to sit on a rigid seat mounted on a sled, and the sled slid on inclined rails from the top to the end. At the end of the rails, an energy-absorbing device caught the sled to generate the given deceleration of the subject as illustrated in Figure 5.

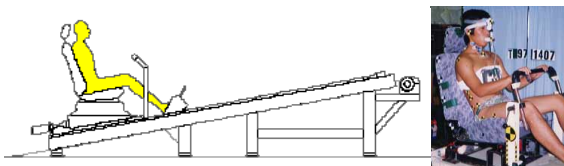


**Figure 5. Slope-type sled test set-up and volunteer.**

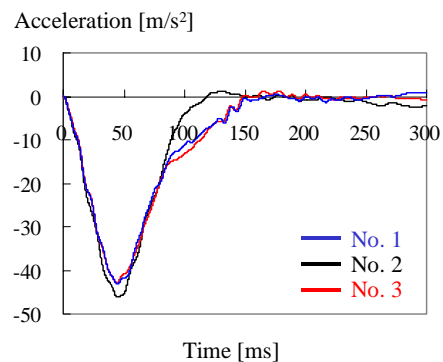
The slope angle was 10 degrees and the initial height was adjusted so that the delta-V (velocity just before the impact) was eight km/h. Test runs were repeated several times so that the subject is relaxed enough. For a direct and simple comparison, three cases without the head-restraint were selected from a series of volunteer tests.

### Test Results

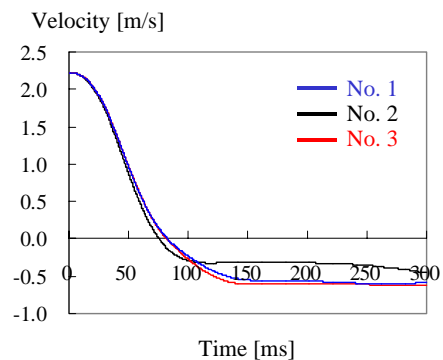
In this test, the behavior of an occupant in low-speed rear-end collision, i.e. the mechanism of whiplash injuries could be reproduced. One of features

in neck kinematics in whiplash can be perceived to be S-shape motion due to the push from the rigid seat and the stretch of vertebral column. The feature in head kinematics can be recognized as the complex acceleration in the both longitudinal and vertical directions due to the S-shape neck motion.

Figure 6 shows the acceleration and the velocity of the sled, Figure 7 (a) and (b) show the accelerations at T1 and Figure 7 (c) and (d) show the accelerations at Sternum. Acceleration due to the rear impact was translated into the acceleration toward frontal direction. In order to specify the velocity boundary conditions, deceleration data were transferred to velocity data by integrating on local axes with respect to time. Rotational motion of the torso was simulated by plural translations at T1, T6 and Sternum. Average data were calculated from the test data of three



(a) Acceleration of SLED.



(b) Velocity of SLED.

**Figure 6. Test results I that will be applied as boundary condition in complete upper model.**

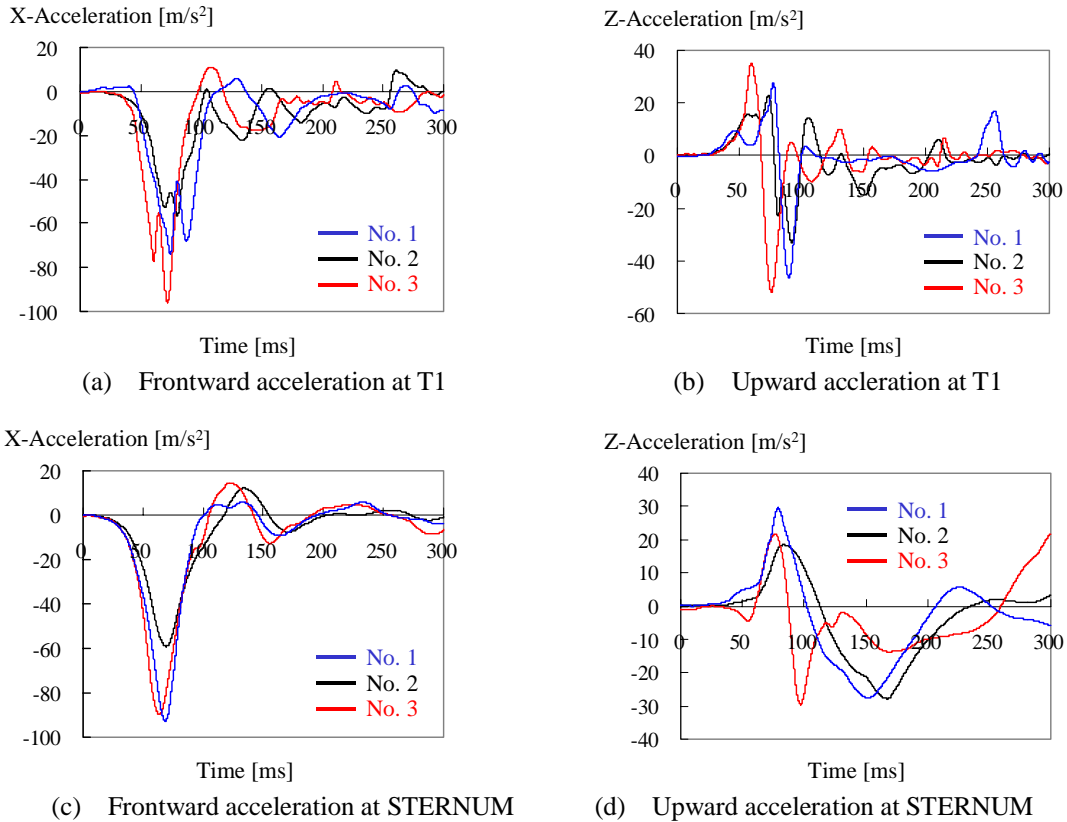


**Figure 7. Test results II that will be applied as boundary condition in simplified neck model.**

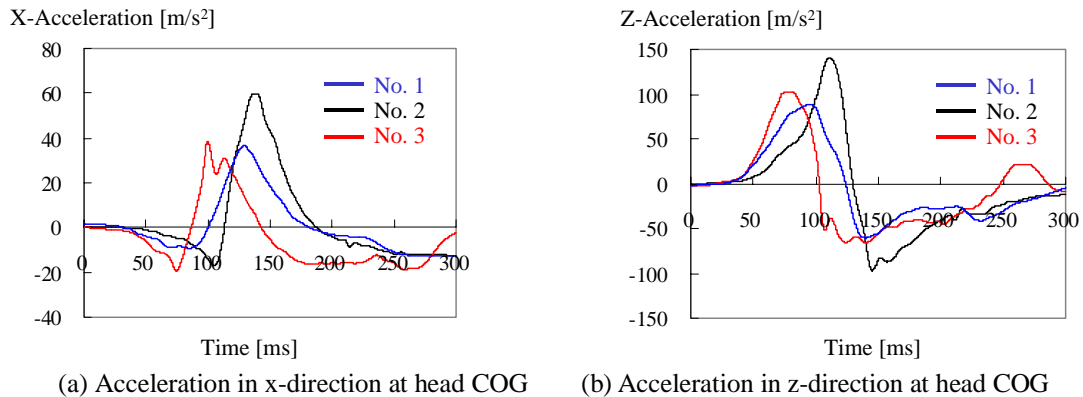


**Figure 8. Test results that should be compared with simulation results.**

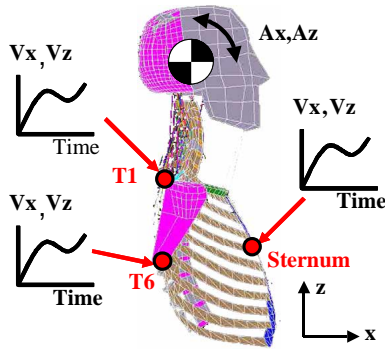
cases in order to apply input data as their functions to the model.

Figure 8-(a) and (b) represent the resultant acceleration at head COG (center of gravity) toward x-direction and z-direction in the coordinate system located at head COG respectively.

### Simulation Model

Figure 9 illustrates the boundary conditions defined on the neck model in order to simulate the rear impact tests. Since the simplified neck model was used

in the first step of this study instead of the entire body model, boundary conditions were directly induced on the model. The first focus of this validation is to reproduce the head-neck responses with respect to the torso motion induced by rear impacts, as illustrated in Figure 9. The head motion at COG should be, therefore, monitored under the given boundary conditions on T1, T6 and Sternum.



**Figure 9. Definition of input on B.C. to partial model.**

In the definition of mechanical response functions for muscle elements, the activity factor  $N_a(t)$  was assumed to be constant during the impact regardless of a reflex time. Based on this assumption, four different states were considered in the following parametric study with respect to the values,  $N_a(t) = 0.005, 0.1, 0.5$  and  $1.0$ . It was assumed that the state with  $N_a(t) = 0.1$  is a basis for muscles in a living human. Considering slight activity of the neck muscles to keep the head straight up,  $N_a(t) = 0.5$  was assumed for dominant muscles in flexion and extension motions (flexors and extensors) as shown in Figure 10.

The complete upper body motion was simulated in the second step on this study, by modeling the rigid seat system mounted on the sled. In this upper body model, the neck muscle modeling method revised in the above partial model is introduced into the base human body instead of solid and shell muscle elements. As simulation results to evaluate and revise the model,

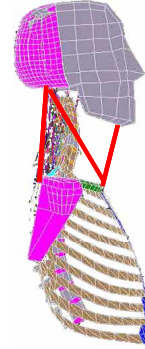


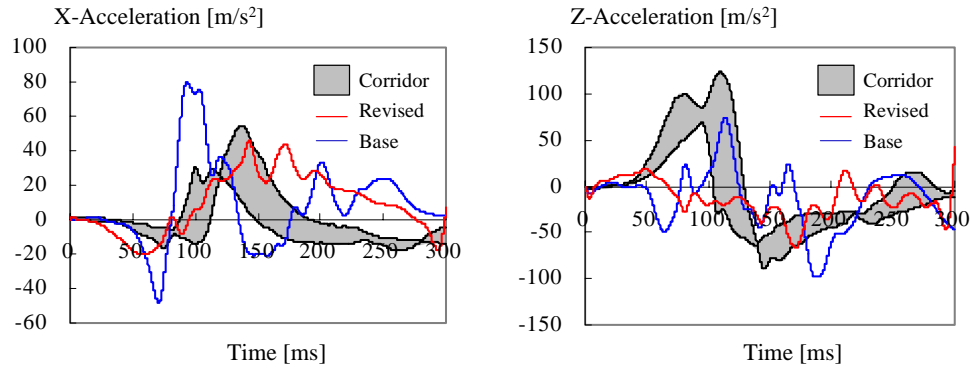
**Figure 10. Characterization of muscle properties.**

the head motion at COG should be monitored under the contact of the upper body with the seat back in the same way of the partial model analysis.

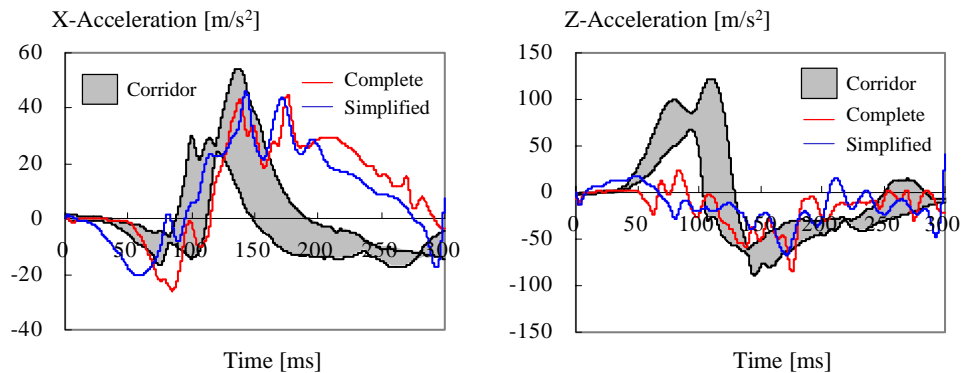
### Simulation Results

Figure 11 compares in acceleration at the head COG between the test results and the simulation results of the simplified neck model shown in Figure 2. Test results were shown as corridors for x-direction (horizontal) and z-direction (vertical). The calculated responses were also compared between the revised model and the base model with same boundary conditions. The test result in x-direction acceleration shows a slight negative peak in early phase and a prominent positive peak between 100 to 150 ms. The tendency of the response curve calculated by the revised model matches well with the test corridor, while the base model generates higher peaks both in negative and positive directions. The test result in z-direction acceleration shows a positive peak during the first half and a negative peak in the second half. The simulation results show a slight mismatch both of the base and the revised model. The revised model does not show a positive peak during the first half while the timing of peak is late in the base model result. In the second half, the revised model matches better with the test corridor than the base model.

Figure 12 shows accelerations at the head



**Figure 11. Validation results of head COG responses in simplified neck model.**



**Figure 12. Validation results of head COG responses in complete upper body model.**

COG in the simulation results of the complete upper body compared with the test results that represented by the corridors. The calculated responses were also compared between the complete upper body model and the simplified neck model in which same spring-dashpot muscle elements were introduced. These simulation results of the acceleration in x-direction match well with the test corridor except the higher response level in the later half compared to that of test result. In complete upper body model, direct contact condition between upper body and sled seat was reproduced, so that the timing of each peak in response curve approached that of test result. Therefore, the tendencies of the response curves calculated by the complete upper body model are similar to those of the simplified neck model analysis, since the same method to represent the neck muscles is adopted in both models.

In addition to checking the head responses, kinematics of the cervical vertebrae (C1 – C7) was also verified. Figure 13 shows time history curves of rotational angle at the vertebra bodies. The simulation results show that the trailing absolute angle curve of the upper vertebra denotes a slight negative peak in the first half phase and a prominent positive peak in the second half phase. A similar tendency was observed in the lower vertebra but the magnitudes of both peaks were smaller. On the other hand, the trailing relative angle curve of each vertebra indicates a slight negative peak in the first half phase and the prominent positive peak in the second phase. They had a similar tendency but the magnitude of positive peak was independent of the position of cervical vertebrae.

Combination of such rotational motions of the vertebrae generated an S-shape motion in the cervical spine, which is known as a typical neck behavior in rear

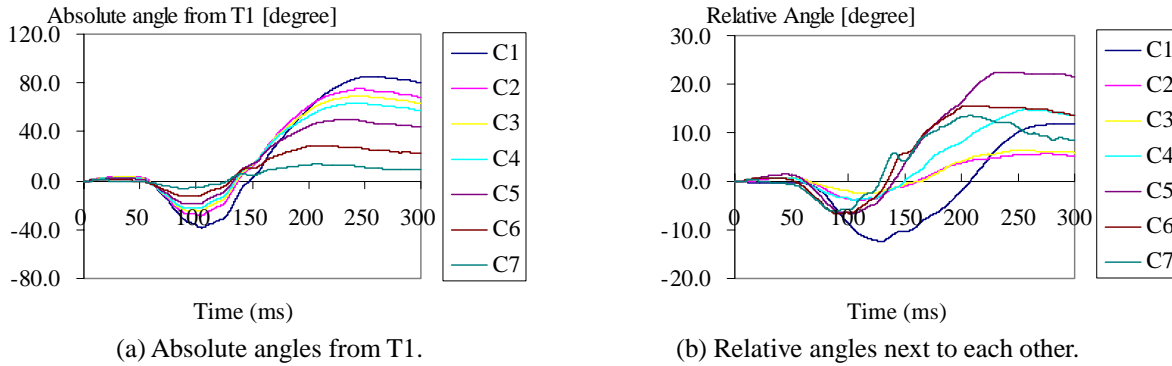


**Figure 13. Validation results of head COG responses in complete upper body model.**

impacts. The results suggest that the model showed reasonable responses to simulate volunteer tests.

## DISCUSSION

Summarizing the comparisons, the revised neck model shows closer responses to the test results compared to the base neck model, especially in x-direction. The complete upper body model with the contact between the upper body and the sled seat gives a better match with the test corridor. These results suggest that the idea of using spring-dashpot elements with the Hill-type algorithm is valid to simulate muscle responses in a living human.

It was confirmed that the revised neck model and complete upper body model with the new muscle elements could be beneficial to simulate the head-neck kinematics and responses during the early phase in a rear impact when retraction occurs. The model should be, however, improved for its response in z-direction. In this case, z-direction indicates the moving direction in the axis of head COG which is rotating, but the upward direction in the global axis. Hence, it is important to remind that the direction of the applied load to the head COG largely depends on the neck shape. In addition to this, it is important to reproduce the subject test condition i.e., the posture in the moment of rear impact. Although we tried to reproduce it carefully, it would be useful to consider the influence of the above condition

upon the head motion in order to improve the simulation results.

## CONCLUSION

The developed human neck model with muscles of spring-dashpot elements has shown good agreement with the volunteer test data in low-speed rear-end impact simulation. However, the head COG acceleration in upward direction of local coordinate system in the head is underestimated. In order to improve the model responses, a detailed consideration and modeling of the contact between the sled seat and the upper body, i.e. the posture of human model is required so as to reproduce an actual phenomenon in the test. Additionally, the possibility of application to different test conditions such as cadaver test would be expected based on the concept of the neck muscle modeling in this successful study.

## ACKNOWLEDGMENTS

The authors wish to thank Laboratoire d'Accidentologie et de Biomecanique (LAB) for the collaborative study and also acknowledge the conduct of experimental collaboration of Japan Automobile Research Institute (JARI).

## REFERENCES

- [1] McConnel, W.E., Howard, R.P., Van Poppel, J., Krause, R., Guzman, H. M., Bomar, J. B, Benedict, J. V. and Hatsell, C. P. 1995. "Human Head and Neck Kinematics after Low Velocity Rear-End Impacts – Understanding 'Whiplash'." In Proceedings of 39th Stapp Car Crash Conference. 215-238.
- [2] Matsushita, T., Ymazaki, N., Sato, T. and Hirabayashi, K. 1997. "Biomechanical and Medical Investigations of Human Neck Injury in Low Velocity Collision." *Neuro-Orthopaedics*, Vol.21, 27-45.
- [3] Ono, K., Kaneoka, K., Wittek, A. and Kajzer, J. 1997. "Cervical Injury Mechanism Based on the Analysis of Human Cervical Vertebral Motion and Head-Neck-Torso Kinematics During Low Speed Rear Impacts." In Proceedings of 41st Stapp Car Crash Conference. 399-356.
- [4] Pope, M. H., Magnusson, M., Alksiev, A., Hasselquist, L., Spratt, K., Szpalski, M., Goel, V. K. and Panagiotacopoulos N. 1998. " Electromyographic Changes Under Whiplash Loading." In *Frontiers in Head and Neck Trauma*, IOS Press, 338-343.
- [5] van der Hors, M. J., Thunnissen, J. G. M., Happee, R. and Wismans, J. 1997. "The Influence of Muscle Activity on Head-Neck Response During Impact." In Proceedings of 4th Stapp Car Crash Conference. 487-507.
- [6] Wittek, A. and Kajzer, J. 1997. "Modeling of Muscle Influence on the Kinematics of the Head-Neck Complex in Impacts." *Memoirs of the School of Engineering, Nagoya University*, Vol. 49, 155-205.
- [7] Wittek, A., Ono, K. and Kajzer, J. 1999. "Application of Modified Neck Model by Nitshe in Investigation of Kinematic Responses of Cervical Spine in Low-Speed Rear-End Collisions: Effect of Muscle Activity." In Proceedings of 1999 PAM User Conference in Asia (PUCA '99). 433-448.
- [8] PAM-SYSTEM SOLVER NOTES Manual. 2000, Level 18, PAM SYSTEM INTERNATIONAL.